2016 IEEE/RSJ International Conference on Intelligent Robots and Systems (IROS)
Daejeon Convention Center
October 9-14, 2016, Daejeon, Korea

Influence of the Magnetic Field on the Two-Dimensional Control of *Magnetospirillum Gryphiswaldense* Strain MSR-1

Heba A. Hassan*, Marc Pichel†, Tijmen Hageman†, Leon Abelmann†‡ and Islam S. M. Khalil*

***Abstract*— Magnetotactic bacteria have the potential to controllably reach deep-seated regions of the body via vessels and achieve targeted drug delivery. In this application, motion of the magnetotactic bacteria is influenced by the strength of the external magnetic field. Here, we investigate the swimming characteristics of magnetotactic bacteria (*Magnetospirillum gryphiswaldense* strain MSR-1) under the influence of uniform and adaptive magnetic fields inside microfluidic chip with depth of 5 μm. This depth enables tracking of single bacterium and comparison of uniform and adaptive magnetic field on the positioning accuracy. We find that under the influence of magnetic field reversal with approximately twice the field strength, the diameter of the *U-turn* trajectories taken by the magnetotactic bacteria is decreased by 63%. In addition, the adaptive magnetic field decreases the size of region-of-convergence of the controlled bacteria within the vicinity of the reference position by 65.5%, compared to control using uniform magnetic field. The comparisons between motion control using uniform and adaptive magnetic fields are done on the same culture of magnetotactic bacteria and using the same cell in each motion control trial.**

I. INTRODUCTION

Magnetotactic bacteria (MTBs) hold promise in targeted drug delivery. These microorganisms have the potential to controllably navigate throughout the human circulatory system and reach deep-seated regions. Their size, magnetic properties, and motility enable high precision motion control using an external magnetic field *only* for directional control. The flagellated propulsion of MTBs allows researchers to use weak magnetic field (millitesla range) for steering without relatively large magnetic field gradient. Martel *et al.* have demonstrated the directional control of swarm of MTBs (magnetotactic coccus strain MC-1) and single bacterium [1], [2]. In addition, this strain has been used to achieve micro-actuation [3] and micro-assembly [4], [5] of non-magnetic beads and objects, respectively. Khalil *et al.* have also demonstrated open- and closed-loop control of MTBs (*Magnetospirillum Magnetotacticum* Strain MS-1 and *Magnetospirillum Magneticum* Strain AMB-1) inside capillary tubes and microfluidic channels with structure of a maze [6], [7]. In addition, a comparative study between MTBs and self-propelled microjets has proven that MTBs are more efficient than microjets (MTBs have an average swimming speed of approximately 6 body lengths per second, whereas microjets swim at approximately 2 body lengths per second) [8]. Kim *et al.* have also demonstrated control of *Tetrahymena Pyriformis* cells in three-dimensional space using two sets of Helmholtz coils and single electromagnet to control the planar and vertical motion of these cells, respectively [9]. A null-space control has also been proposed in [10], and the accuracy of the motion control is increased by projecting an additional control input onto the null space of the magnetic

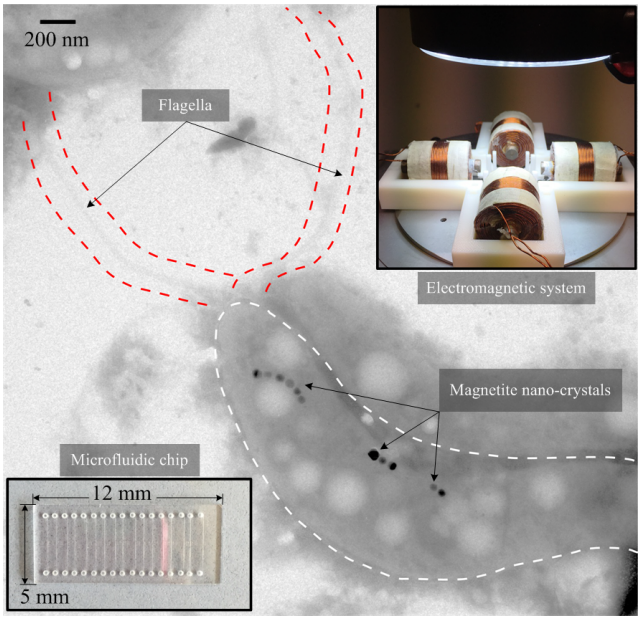

Fig. 1. Transmission Electron Microscopy image of a magnetotactic bacterium (MTB), i.e., *Magnetospirillum gryphiswaldense* strain MSR-1. The cell and flagella of the bacterium are indicated using the dashed white and red lines, respectively. The magnetite nano-crystals allow the MTB to align along external magnetic field lines and swim using its flagella. Magnetotactic bacteria (MTBs) are contained inside microfluidic chips (bottom-left corner) with depth of 5 μm. The chip is surrounded with electromagnetic coils (upper-right corner) to enable directional control of the MTB in two-dimensional space under microscopic guidance, using maximum magnetic field of 10 mT. The depth of the chip does not allow the MTB to swim out-of-plane, and hence the effect of the controlled magnetic field is studied on the same bacterium. The average diameter and length of the MTBs are calculated to be 240±6 nm and 5±0.2 μm, respectively.

This work was supported by funds from the German University in Cairo and the DAAD-BMBF funding project. The authors also acknowledge the funding from the Science and Technology Development Fund in Egypt (No. 23016).

*German University in Cairo, New Cairo 11835, Egypt.
†Korean Institute of Science and Technology, Saarland University, Saarbrücken 66111, Germany.
‡Leon Abelmann is affiliated with MESA+ Institute for Nanotechnology, University of Twente, 7500 AE Enschede, The Netherlands.

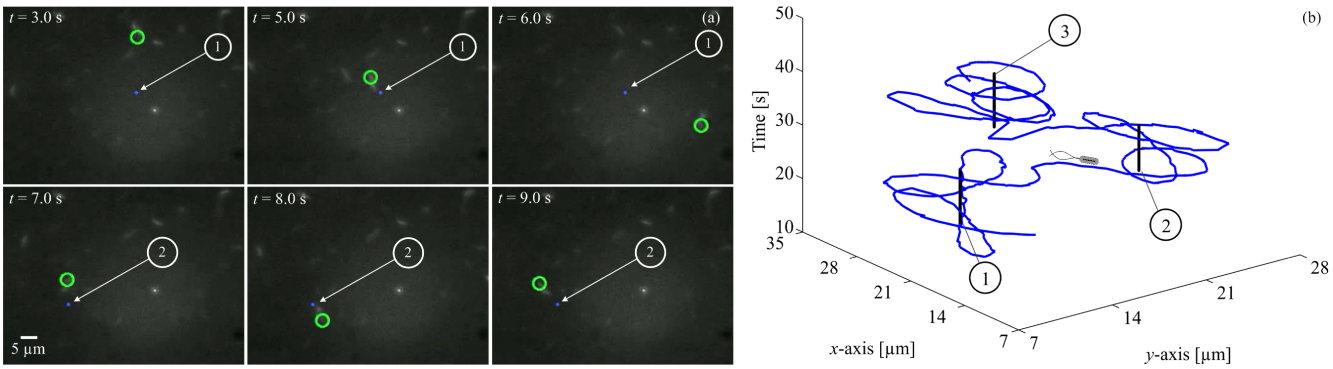

Fig. 2. A representative closed-loop control of a magnetotactic bacterium (MTB), i.e., *Magnetospirillum gryphiswaldense* strain MSR-1, under the influence of the controlled magnetic fields. (a) The closed-loop control system localizes the MTB within the vicinity of the reference position (small blue circle). (b) Three reference positions (vertical black lines) are given to the control system and the MTB is localized within their vicinity. The diameter of the region-of-convergence of the three reference positions are 51 μm, 38.9 μm, and 38.2 μm. The speed of the MTB is calculated to be 24.7 μm/s, in this trial. The green circle indicates the position of the MTB. *Please refer to the accompanying video that demonstrates the closed-loop proportional control of an MTB.*

force-current map of a configuration of electromagnetic coils. The projection of this additional control input enables oscillation of the magnetic fields and directional control towards a reference position to decrease the speed of the MTBs within the vicinity of the reference position. Although this null-space control strategy decreases the region-of-convergence of the controlled MTBs within the vicinity of the reference position, the generation of oscillating magnetic fields may have adverse effects on the electromagnetic coils. The alternating current causes the coils to heat up and decreases their availability, for instance. In this study we achieve the following:

- Study the influence of the magnetic field strength on the positioning accuracy of MTBs. This study is done by applying different magnetic fields on the same bacterium from the same culture, in each trial;
- A comparative study between closed-loop motion control using uniform magnetic field and adaptive magnetic field with the position tracking error.

We present a control strategy to increase the positioning accuracy of the magnetotactic bacterium (MTB) using an adaptive magnetic field. The adaptation is accomplished based on the magnitude of the error of the MTB with respect to the reference position. In addition, we study the influence of the magnetic field [11], [12], [13] on the closed-loop control characteristics of the MTB, and conduct comparative control trials using two control systems on the same bacterium (in each trial), inside microfluidic chip that does not enable MTBs to swim out-of-plane.

The remainder of this paper is organized as follows: Section II provides modeling of the MTB, design of a proportional motion control system, and its error dynamics based on passivity analysis. Motion control of MTB inside microfluidic chips using uniform and adaptive magnetic fields are provided in Section III. Finally, Section IV concludes and provides directions for future work.

II. MODELLING AND MOTION CONTROL OF MAGNETOTACTIC BACTERIA

Under the influence of external magnetic field in two-dimensional space, an MTB is subjected to the following magnetic force ($\mathbf{F} \in \mathbb{R}^{2\times1}$) and magnetic torque ($\mathbf{T} \in \mathbb{R}^{2\times1}$):

$$\begin{pmatrix}\mathbf{F}\\ \mathbf{T}\end{pmatrix} = V\begin{pmatrix}(\mathbf{m}\cdot\nabla)\,\mathbf{B}(\mathbf{P})\\ \mathbf{m}\times\mathbf{B}(\mathbf{P})\end{pmatrix} = V\begin{pmatrix}(\mathbf{m}\cdot\nabla)\,\mathbf{B}(\mathbf{P})\\ \hat{\mathbf{m}}\mathbf{B}(\mathbf{P})\end{pmatrix}, \quad (1)$$

where V is the volume of the magnetite (Fe_3O_4) nanocrystals that are contained inside the cell of the MTB, as shown in Fig. 1. Further, $\mathbf{m} \in \mathbb{R}^{2\times1}$ and $\mathbf{B}(\mathbf{P}) \in \mathbb{R}^{2\times1}$ are the magnetization (magnetic moment per volume) and the induced magnetic fields at point ($\mathbf{P} \in \mathbb{R}^{2\times1}$), respectively. Our MTBs are contained inside microfluidic chips with depth of 5 μm (equal to the depth of focus of the microscopic system). Therefore, the MTBs do not undergo out-of-plane swimming, and we can assume planar motion ($\mathbf{B}(\mathbf{P}) \in \mathbb{R}^{2\times1}$). In (1), $\hat{\mathbf{m}}$ is the skew-symmetric form of the magnetization vector ($\mathbf{m}$), where $\hat{\mathbf{m}} = \mathrm{SK}(\mathbf{m})$, and $\mathrm{SK}(\cdot)$ is the skew-symmetric operator [14]. An MTB navigates in a viscous flow and experiences drag force ($\mathbf{f} \in \mathbb{R}^{2\times1}$) and drag torque ($\mathbf{t} \in \mathbb{R}^{2\times1}$) that are approximated by [15], [16]

$$\begin{pmatrix}\mathbf{f}\\ \mathbf{t}\end{pmatrix} = -\begin{pmatrix}a & b\\ b & c\end{pmatrix}\begin{pmatrix}\mathbf{v}\\ \omega\end{pmatrix}, \quad (2)$$

where $\mathbf{v} \in \mathbb{R}^{2\times1}$ and $\omega \in \mathbb{R}^{2\times1}$ are the linear and angular velocity vectors of the MTB, respectively. Further a, b, and c are the coefficients of the propulsion matrix and are given by

$$a = 2\pi n R_{\mathrm{h}}\left(\frac{\xi_{\parallel}\sin^2\theta + \xi_{\perp}\cos^2\theta}{\cos\theta}\right). \quad (3)$$

In (3), n and R_{h} are the number of turns of the helical flagella and the radius of the helix. Further, θ is the helix angle, and

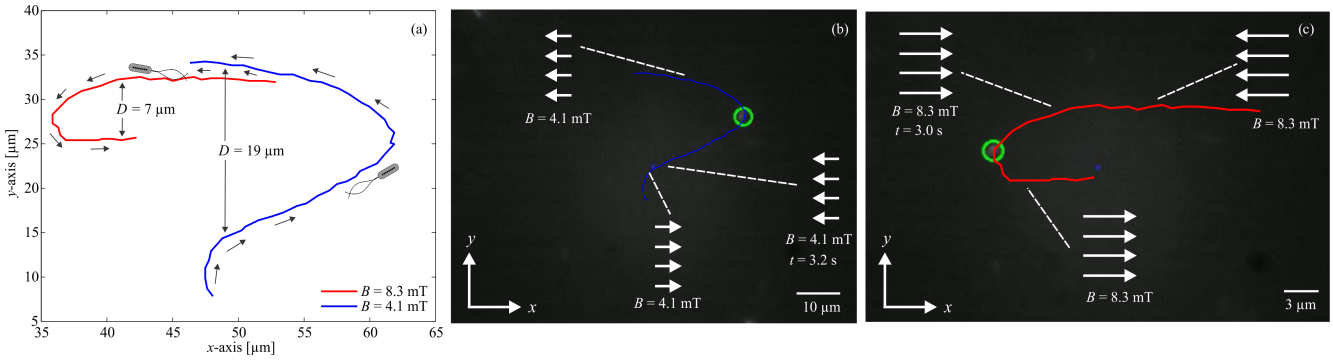

Fig. 3. A representative *U-turn* experiment of a magnetotactic bacterium (MTB), i.e., *Magnetospirillum gryphiswaldense* strain MSR-1, under the influence of magnetic field reversals. (a) This trial is done using the same MTB. The *U-turn* experiment is done at 2 magnetic fields, i.e., 4.1 mT and 8.3 mT. (b) Uniform magnetic field of 4.1 mT is applied and at time, t=3.2 seconds, the field is reversed. The MTB undergoes a *U-turn* (blue line) with diameter of 19 μm. (c) Uniform magnetic field of 8.3 mT is applied on the same bacterium and at time, t=3.0 seconds, the field is reversed. The MTB undergoes a *U-turn* (red line) with diameter of 7 μm. *Please refer to the accompanying video that demonstrates the U-turn trajectories taken by the same MTB under the influence of two magnetic field reversals with magnitudes of 4.1 mT and 8.3 mT.*

the drag coefficients ($\xi_{\parallel}$) and ($\xi_{\perp}$) are given (respectively) by

$$\xi_{\parallel} = \frac{4\pi\eta a}{\ln\left(\frac{2a}{b}\right) - \frac{1}{2}} \quad \text{and} \quad \xi_{\perp} = \frac{8\pi\eta a}{\ln\left(\frac{2a}{b}\right) + \frac{1}{2}}, \tag{4}$$

where a and b are the length and diameter of the cell of the MTB. The average diameter and average length of the *Magnetospirillum gryphiswaldense* strain MSR-1 are calculated to be 240±6 nm and 5±0.2 μm, respectively. Further, η is the dynamic viscosity of the growth medium. In (2), b is given by [15]

$$b = 2\pi n R_{\mathrm{h}}^2 \left(\xi_{\parallel} - \xi_{\perp}\right) \sin\theta. \tag{5}$$

Finally, c is calculated using [15]

$$c = 2\pi n R_{\mathrm{h}}^3 \left(\frac{\xi_{\parallel}\cos^2\theta + \xi_{\perp}\sin^2\theta}{\cos\theta}\right). \tag{6}$$

Our motion control strategy is based on directing the magnetic field lines towards a reference position. Therefore, we use the rotational dynamics of the MTB to analyze and design the control input. Using (1) and (2), we obtain the following rotational dynamics of an MTB:

$$V\hat{\mathbf{m}}\mathbf{B}(\mathbf{P}) - b\mathbf{v} - c\omega = 0. \tag{7}$$

The magnetic field ($\mathbf{B}(\mathbf{P})$) is controlled to align the MTB towards a reference position. Therefore, the angular position and velocity errors ($\mathbf{e}$ and $\dot{\mathbf{e}}$) are given by

$$\mathbf{e} = \Phi - \Phi_{\mathrm{ref}} \quad \text{and} \quad \dot{\mathbf{e}} = \dot{\Phi} = \omega, \tag{8}$$

where Φ and Φ_{ref} are the angular position of the MTB and the fixed reference orientation that directs the MTB towards the reference position, respectively. We rewrite (7) using (8), and devise a proportional control input ($\mathbf{B}(\mathbf{P}) \mapsto \mathbf{K}_{\mathrm{p}}\mathbf{e}$) to obtain the following error dynamics:

$$\dot{\mathbf{e}} - \frac{V}{c}\hat{\mathbf{m}}\mathbf{K}_{\mathrm{p}}\mathbf{e} = -\frac{b}{c}\mathbf{v}, \tag{9}$$

where $\mathbf{K}_{\mathrm{p}}$ is a positive-definite matrix. We select the following storage function $S(\mathbf{e})$:

$$S(\mathbf{e}) = \frac{1}{2}\mathbf{e}^{\mathrm{T}}\mathbf{e}. \tag{10}$$

Taking the time-derivative of (10) yields

$$\dot{S}(\mathbf{e}) = \frac{V}{c}\mathbf{e}^{\mathrm{T}}\mathbf{K}_{\mathrm{p}}^{\mathrm{T}}\hat{\mathbf{m}}^{\mathrm{T}}\mathbf{e} - \frac{b}{c}\mathbf{v}^{\mathrm{T}}\mathbf{e} \leq -\frac{b}{c}\mathbf{v}^{\mathrm{T}}\mathbf{e}. \tag{11}$$

Therefore, the system with the input (-$\mathbf{v}$) and output ($\mathbf{e}$) is passive with the storage function ($S(\mathbf{e})$). We implement two control strategies and compare the motion characteristics of the MTBs. The first control strategy is based on uniform magnetic fields, whereas the second strategy depends on adapting the magnetic field based on the position error. The same culture of MTBs is used in each case to study the influence of the control on the closed-loop motion characteristics. *Magnetospirillum gryphiswaldense* strain MSR-1 is obtained from the German collection of microorganisms and cell cultures (DSM 6361, Deutsche Sammlung von Mikro-organismen und Zellkulturen, Brunswick, Germany). The strain is inoculated in magnetospirilum growth medium with an oxygen concentration of 1%. The cultures are then cultivated at 26°C for two to four days. The samples are harvested and selected for experiments based on the presence of individual magnetic chains and their response to external magnetic fields.

Fig. 2(a) provides a representative closed-loop control trial using uniform magnetic fields based on (11). In this trial, the MTB swims at an average speed of 24.7 μm/s, and the maximum region-of-convergence is calculated to be 51 μm, within the vicinity of the first reference position ①. The region-of-convergence is calculated at the steady-state and represents the maximum peak-to-peak amplitude with respect to the reference position (vertical black lines). This closed-loop control trial shows that the magnetic fields successfully orient the MTB towards the reference position and enables localization within the vicinity of the three reference positions (①, ②, and ③), as shown in Fig. 2(b). Although the

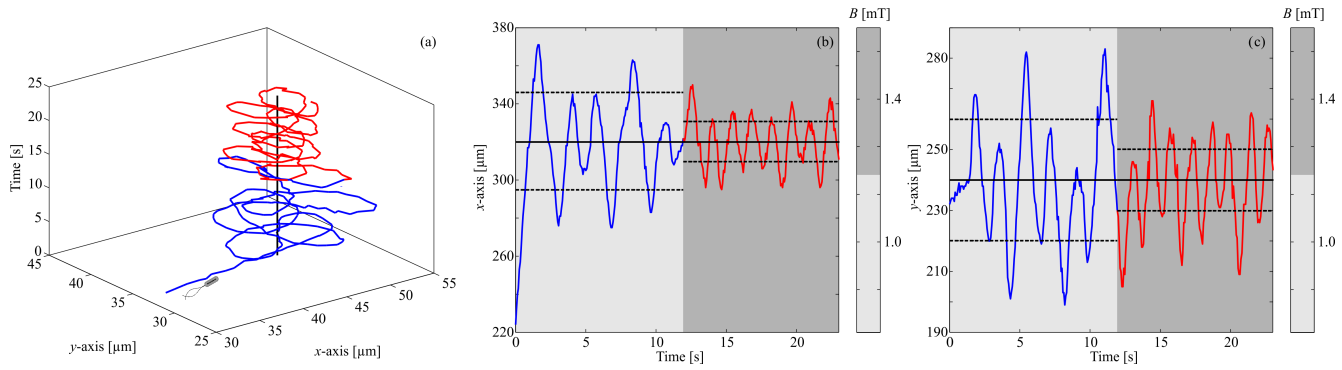

Fig. 4. The influence of the magnetic field on the size of the region-of-convergence is analyzed on the same magnetotactic bacterium (MTB), i.e., *Magnetospirillum gryphiswaldense* strain MSR-1, by increasing the magnitude of the magnetic field. The MTB is localized within the vicinity of the reference position (vertical black line) and the magnetic field is increased from 1.0 mT to 1.4 mT at time, t=12.0 seconds. The size of the region-of-convergence is decreased from 18.4 μm to 11.3 μm. The red and blue lines indicate the path of the MTB under the influence of the magnetic fields of 1.0 mT and 1.4 mT, respectively. (a) The path taken by the controlled MTB towards the reference position (vertical black line). (b) Position of the MTB along x-axis. (c) Position of the MTB along y-axis. The black dashed lines represent the calculated standard deviation. *Please refer to the accompanying video that demonstrates the response of an MTB to magnetic fields with different magnitudes.*

MTB is controlled and its motion is localized within the vicinity of the reference positions, the size of the region-of-convergence is relatively large (10 times greater than a body-length). The region-of-convergence can be decreased to increase the accuracy of localization. This decrease is done by increasing the magnitude of the applied magnetic field. We observe that the MTB undergoes *U-turn* trajectories within the vicinity of the reference positions, as shown in Fig. 2, due to the multiple field reversals of the closed-loop control system to decrease the position error based on (11). The diameter (D) of the *U-turn* trajectory is given by [17]

$$D = \frac{\alpha\pi \mid \dot{\mathbf{P}} \mid}{\mid \mathbf{m} \mid\mid \mathbf{B}(\mathbf{P}) \mid}, \tag{12}$$

where α is the rotational drag coefficient of the MTB, and is approximated using [13]

$$\alpha = \frac{\pi\eta a^3}{3}\left[\ln\left(\frac{a}{b}\right) + 0.92\left(\frac{b}{a}\right) - 0.662\right]^{-1}. \tag{13}$$

Equation (12) indicates that increasing the magnetic field decreases the diameter of the *U-turn* trajectory, and hence reduces the size of the region-of-convergence of a controlled MTB. Fig. 3 demonstrates the effect of the magnitude of the magnetic field on the diameter of the *U-turn* of the same bacterium. At magnetic field of 4.1 mT, the MTB undergoes a *U-turn* with diameter of 19 μm after the reversal of the magnetic field. Increasing the magnitude of the magnetic field to 8.3 mT causes the *U-turn* diameter to decrease to 7 μm, for the same MTB. The magnetic field is calculated using a finite-element model [10], and this model is verified using a calibrated 3-axis digital Teslameter (Senis AG, 3MH3A-0.1%-200 mT, Neuhofstrasse, Switzerland). We repeat this experiment 5 times on different MTBs and observe consistent decrease in the *U-turn* diameter with the increasing magnetic field. We find that under the influence of magnetic field reversal with approximately twice the field strength, the diameter of the *U-turn* trajectories taken by the MTBs is decreased by 63%. Therefore, we design a closed-loop control system based on this observation to enable reduction of the region-of-convergence.

III. CONTROL OF MTBs USING UNIFORM AND ADAPTIVE MAGNETIC FIELDS

The size of the region-of-convergence can be decreased using an adaptive magnetic field that depends on the magnitude of the error. First, we study the influence of the magnetic field on the positioning accuracy of the MTBs. The magnetic field is increased from 1.0 mT to 1.4 mT, as shown in Fig. 4. In this representative experiment, the MTB is controlled at magnetic field of 1.0 mT towards a fixed reference position (Fig. 4(a)). The magnetic field is increased at time, t=12 seconds, from 1.0 mT to 1.4 mT. The region-of-convergence is calculated to be 18.4 μm and 11.3 μm for magnetic fields of 1.0 mT to 1.4 mT, respectively. The blue and red lines represent the path taken by the MTB under the influence of magnetic fields of 1.0 mT and 1.4 mT, respectively. Figs. 4(b) and (c) indicate that increasing the magnetic field by 40% achieves 38.5% reduction in the region-of-convergence of the controlled MTB.

We repeat this experiment 6 times on 6 different MTBs (from the same culture) and increase the magnetic field on each controlled MTB. The corresponding region-of-convergence for each MTB is shown in Fig. 5. These control trials indicate that the magnitude of the applied magnetic field decreases the size of the region-of-convergence regardless to the magnetic properties of the MTB. An MTB with greater (e.g., MTB_6) dipole moment can be localized within a smaller region-of-convergence under the influence of lower magnetic fields. The influence of the magnetic dipole moment of the MTBs on the size of the region-of-convergence is qualitatively shown in Fig. 6, at a uniform magnetic field of 1.4 mT. The magnetic dipole is calculated using (12) for 6 different MTBs from the same culture. This result indicates that an MTB with larger magnetic dipole moment is

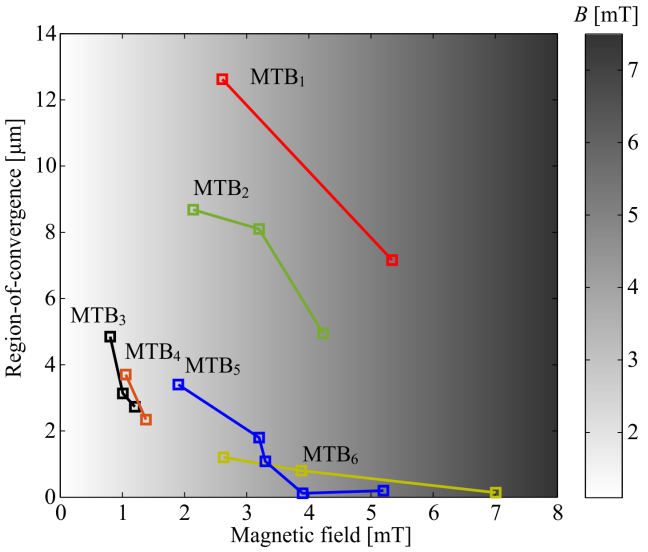

Fig. 5. Closed-loop control of magnetotacitic bacteria (MTBs) at different magnetic fields is achieved. Increasing the magnitude of the magnetic fields results in a decrease in the region-of-convergence of the controlled magnetotactic bacterium (MTB) and does not have an influence on its swimming speed. The 6 closed-loop control trials are done using MTBs from the same culture (*Magnetospirillum gryphiswaldense* strain MSR-1). Each trial is done using the same MTB.

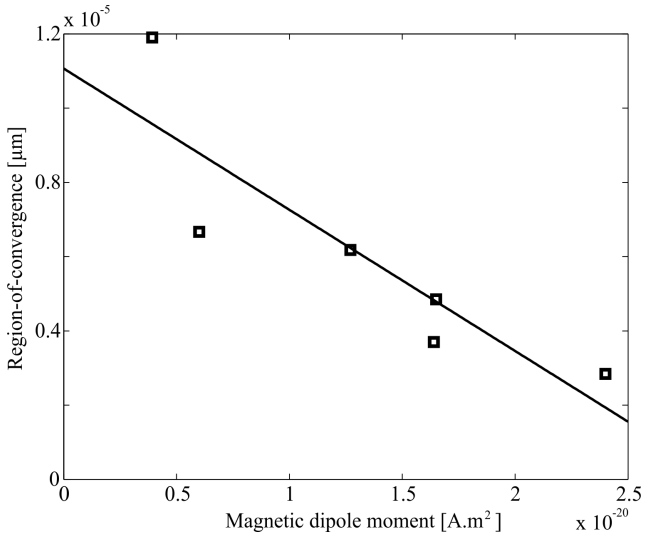

Fig. 6. The influence of the magnetic dipole moment on the positioning accuracy of magnetotactic bacteria (MTBs). This experiment provides a qualitative information pertaining to the influence of the magnetic dipole moment of the MTBs (*Magnetospirillum gryphiswaldense* strain MSR-1) on their positioning accuracy in terms of region-of-convergence. The bacterium with relatively large dipole moment achieves smaller region-of-convergence under the influence of the same control and magnetic field strength. The magnetic dipole moment is calculated using (12), at magnetic field of 1.4 mT for 6 different MTBs from the same culture.

localized within a smaller region-of-convergence, compared to another MTB with lower magnetic dipole, at the same magnetic field. Therefore, its essential to devise a control system that increases the magnitude of the magnetic field with the decreasing error. This adaptation is accomplished by varying the control gains based on the calculated error (8), using the following adaptation law:

$$\mathbf{K}_{\mathrm{p}} = k_1 \exp^{\left(-\frac{\mathbf{e}}{k_2}\Pi\right)} + k_3\Pi, \tag{14}$$

where k_1, k_2, and k_3 are positive control gains, and Π is the identity matrix. The adaptation law (14) allows us to increase the magnetic field strength for errors with relatively small magnitudes. Relatively low magnetic field can be used when the error is large since low torque ultimately allows the MTB to align along the magnetic field lines. Once the error is decreased and the MTB is localized within the vicinity of the reference position, control law (14) increases the magnetic field to decrease the *U-turn* diameter and enables faster reversals and higher positioning accuracy. Fig. 7 provides a representative closed-loop motion control result of an MTB using control law (14). Four reference positions are given to the control system and the MTB swims towards each reference at an average speed of 94.3 μm/s. The region-of-convergence of the 4 reference positions are calculated to be 18.1 μm, 13.9 μm, 12.3 μm, and 14.7 μm, respectively. Although Figs. 2 and 7 provide a qualitative comparison between the control using uniform and adaptive magnetic fields, the difference between the magnetic properties of the MTBs (we use bacteria from the same culture throughout this study) does not enable a fair comparison to be made. Therefore, we implement the two control systems on the same MTB. The average region-of-convergence is calculated to be 42.7$\pm$7 μm and 14.75$\pm$2 μm for the control using uniform and adaptive magnetic fields, respectively. This experiment indicates that a decrease of 65.5% is achieved using the same average magnetic field for the two control systems. *Please refer to the accompanying video that demonstrates the influence of using uniform and adaptive magnetic fields on a controlled MTB.*

Although the adaptive control system achieves a decrease in the size of the region-of-convergence of the controlled MTB, the magnetic properties of the MTBs have greater influence on the positioning accuracy. Fig. 5 shows the difference in region-of-convergence for closed-loop control trials on 6 MTBs. Not only do we observe the influence of the increased magnetic field on the positioning accuracy, but we also find that the magnetic properties of each MTB has a major effect on the control characteristics. The blue (MTB_5) and yellow (MTB_6) lines in Fig. 5 represent control of 2 MTBs with region-of-convergence of less than a body-length, whereas the red (MTB_1) and green (MTB_2) lines represent controlled results of 3 other MTBs with region-of-convergence that is slightly greater than a body-length. Therefore, it is essential to implement closed-loop motion control using adaptive magnetic field with the position error on MTBs with the greatest magnetic dipole moment.

IV. CONCLUSIONS AND FUTURE WORK

In this study, we control the motion of magnetotactic bacteria, *Magnetospirillum gryphiswaldense* strain MSR-1, using uniform and adaptive magnetic fields. In contrast to the

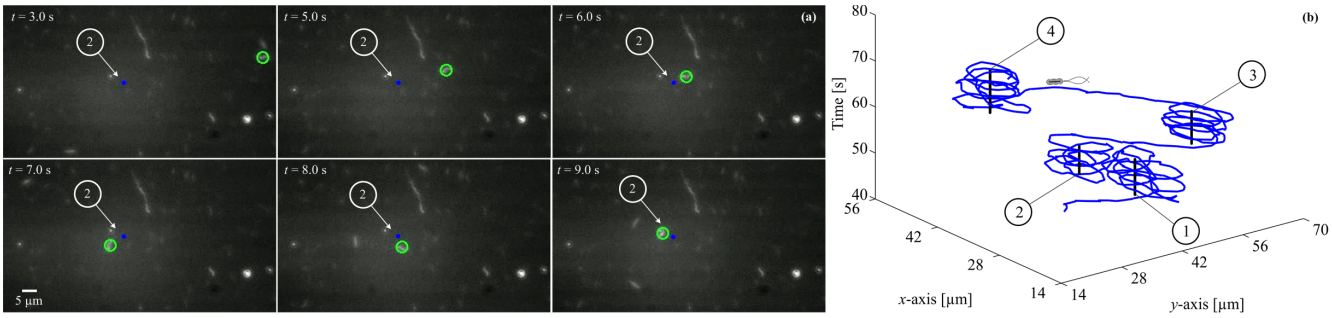

Fig. 7. A representative closed-loop control of a magnetotactic bacterium (MTB), i.e., *Magnetospirillum gryphiswaldense* strain MSR-1, under the influence of the controlled magnetic fields. (a) The closed-loop control system localizes the MTB within the vicinity of the reference position (small blue circle). (b) Four reference positions (vertical black lines) are given to the control system and the MTB is localized within their vicinity. The size of the region-of-convergence are 18.1 μm, 13.9 μm, 12.3 μm, and 14.7 μm. The speed of the MTB is calculated to be 94.3 μm/s, in this trial. The green circle indicates the position of the MTB. *Please refer to the accompanying video that demonstrates our closed-loop adaptive control of an MTB.*

control using uniform magnetic field that achieves localization of an MTB with relatively large region-of-convergence, the adaptive magnetic field enables reduction of the region-of-convergence of the controlled MTBs with 65.5%. This reduction is achieved by increasing the magnitude of the applied magnetic fields as the error between the position of the MTB and the reference position decreases. The motion control using the adaptive magnetic field achieves localization of MTBs with maximum positioning error of 3 body-lengths.

As part of future studies, motion control of magnetotactic bacteria will be achieved inside micro-fluidic channels with controlled time-varying flow rate. This study is necessary to translate these microorganisms into *in vivo* applications. The motion control characteristics will be studied along and against the flowing streams of the growth medium to analyze the ability of the flagellar propulsive force to overcome the force due to time-varying flow and drag [18], [19].

REFERENCES

[1] S. Martel, O. Felfoul, J.-B. Mathieu, A. Chanu, S. Tamaz, M. Mohammadi, M. Mankiewicz, and N. Tabatabaei , "MRI-based medical nanorobotic platform for the control of magnetic nanoparticles and flagellated bacteria for target interventions in human capillaries," *The International Journal of Robotics Research*, vol. 28, no. 9, pp. 1169-1182, September 2009.

[2] I. S. M. Khalil and S. Misra, "Control characteristics of magnetotactic bacteria: *Magnetospirillum magnetotacticum* strain MS-1 and *Magnetospirillum magneticum* Strain AMB-1" *IEEE Transactions On Magnetics,* vol. 50, no. 4 (5000211), April 2014.

[3] Z. Lu and S. Martel, "Controlled bio-carriers based on magnetotactic bacteria," in *Proceedings of The IEEE International Conference on Solid-State Sensors, Actuators and Microsystems*, pp. 683-686, Lyon, France, June 2007.

[4] S. Martel and M. Mohammadi, "Using a swarm of self-propelled natural microrobots in the form of flagellated bacteria to perform complex micro-assembly tasks," in *Proceedings of The IEEE International Conference on Robotics and Automation*, pp. 500-505, Alaska, USA, May 2010.

[5] Z. Lu and S. Martel, "Preliminary investigation of bio-carriers using magnetotactic bacteria," in *Proceedings of The IEEE Engineering in Medicine and Biology Society Annual International Conference (EMBS)*, pp. 683-686, New York City, USA, September 2006.

[6] I. S. M. Khalil, M. P. Pichel, L. Zondervan, L. Abelmann, and S. Misra, "Characterization and control of biological microrobots," in *Proceedings of the 13th International Symposium on Experimental Robotics-Springer Tracts in Advanced Robotics*, Springer Tracts in Advanced Robotics (STAR), vol. 88, pp. 617–631, June 2012.

[7] I. S. M. Khalil, M. P. Pichel, O. S. Sukas, L. Abelmann, and S. Misra, "Control of magnetotactic bacterium in a micro-fabricated maze," in *Proceedings of the IEEE International Conference on Robotics and Automation (ICRA)*, pp. 5488-5493, Karlsruhe, Germany, May 2013.

[8] I. S. M. Khalil, V. Magdanz, S. Sanchez, O. G. Schmidt and S. Misra, "Magnetotactic bacteria and microjets: A comparative study," in *Proceedings of the IEEE/RSJ International Conference of Robotics and Systems (IROS)*, pp. 2035-2040, Tokyo, Japan, November 2013.

[9] D. H. Kim, P. S. S. Kim, A. A. Julius, and M. J. Kim, "Three-dimensional control of engineered motile cellular microrobots," in *Proceedings of the IEEE International Conference on Robotics and Automation (ICRA)*, pp. 721-726, Minnesota, USA, May 2012.

[10] I. S. M. Khalil, M. P. Pichel, L. Abelmann, and S. Misra, "Closed-loop control of magnetotactic bacteria," *The International Journal of Robotics Research*, vol. 32, no. 6, pp. 637-649, May 2013.

[11] K. Erglis, Q. Wen, V. Ose, A. Zeltins, A. Sharipo, P. A. Janmey, and A. Cebers, "Dynamics of magnetotactic bacteria in a rotating magnetic field," *Biophysical Journal*, vol. 93, no. 4, pp. 1402-1412, August 2007.

[12] B. Steinberger, N. Petersen, H. Petermann, and D. G. Wiess, "Movement of magnetic bacteria in time-varying magnetic fields," *Journal of Fluid Mechanics*, vol. 273, pp. 189-211, May 1994.

[13] Y. R. Chemla, H. L. Grossman, T. S. Lee, J. Clarke, M. Adamkiewicz, and B. B. Buchanan, "A new study of bacterial motion: superconducting quantum interference device microscopy of magnetotactic bacteria," *Biophysical Journal*, vol. 76, pp. 3323-3330, June 1999.

[14] M. P. Kummer, J. J. Abbott, B. E. Kartochvil, R. Borer, A. Sengul, and B. J. Nelson, "OctoMag: an electromagnetic system for 5-DOF wireless micromanipulation," *IEEE Transactions on Robotics*, vol. 26, no. 6, pp. 1006-1017, December 2010.

[15] K. E. Peyer, L. Zhang, and B. J. Nelson, "Bio-inspired magnetic swimming microrobots for biomedical applications", *Nanoscale*, vol. 5, no. 4, pp. 1259-1272, November 2012.

[16] E. M. Purcell, "Life at low Reynolds number,"*American Journal of Physics*, vol. 45, no. 1, pp. 3-11, June 1977.

[17] A. S. Bahaj and P. A. B. James, "Characterisation of magnetotactic bacteria using image processing techniques," *IEEE Transactions on Magnetics*, vol. 29, no. 6, pp. 3358-3360, November 1993.

[18] I. S. M. Khalil, V. Magdanz, S. Sanchez, O. G. Schmidt, and S. Misra, "The control of self-propelled microjets inside a microchannel with time-varying flow rates," *IEEE Transactions on Robotics*, vol. 30, no. 1, pp. 49-58, February 2013.

[19] I. S. M. Khalil, H. Abass, M. Shoukry, A. Klingner, R. M. El-Nashar, M. Serry, and S. Misra, "Robust and optimal control of magnetic microparticles inside fluidic channels with time-varying flow rates," *International Journal of Advanced Robotic Systems*, vol. 13, no. 123, June 2016.